JCSE The Journal of Corrosion Science and Engineering
ISSN 1466-8858 Volume 11, Preprint 35 submitted 11 December 2008

Synergistic Effect of Chloride and NO_2 on the Atmospheric Corrosion of Bronze

Cao Xia, [1, 2] Wang Ning [2]*

1. Jiangsu University of Science and Technology, Jiangsu, 212003, China
2. Beijing University of Aeronautics and Astronautics, Beijing, 100083, China

Abstract

The effect of Chloride and NO_2 on the atmospheric corrosion of bronze was thoroughly investigated by using exposure test. Surface tension test and electrochemical impedance measurements together with Scanning Electron microscopy（SEM）with Energy Dispersive Atomic X-ray (EDAX), and X-ray diffraction (XRD) were used to characterize the corrosion product. The results of the weight loss measurement showed that the whole corrosion kinetics can be approximately described by : $W = at^b$. Synergistic effect of chloride and NO2 was obviously observed, however no nitrate existed in the corrosion products. A new catalyst theory was put forward: NO_2 acted as a catalyst during the corrosion process when much chloride was coexisted.

Keyword: Corrosion, Bronze, Chloride+NO_2, Synergism effect, Catalyst

Introduction

The effect of air pollutants and climatic parameters on the atmospheric corrosion of metal and its simulation has been the topics of several fields and laboratory studies [1-4]. It's generally

ISSN 1466-8858 Volume 11, Preprint 35 submitted 11 December 2008

agreed that besides humidity and wetness time, deposition of sulfur dioxide, nitrogen dioxide and Cl^- as well as the pH value of rainfall are major factors determining the corrosion rate of metal. Many researches have focused on the synergism between two of the pollutants[5-11]. It has been found, for example, that at high relative humidity, copper shows SO_2+NO_2 synergisms [9], and that for steel is negligible [10]. For metals with a protecting oxide film, NO_2 may even act as an inhibitor; otherwise, there seems to be synergistic effect [9]. In other works of this paper's author [11], no synergistic effect of simultaneous interaction of SO_2+Cl- with cast iron was observed. However few papers were focused on the synergistic effect of SO_2+Cl- with copper and its alloys.

Among the family of ancient metals, bronzes have been widely studied. Numerous studied on ancient and historic bronze has tried to establish the chemical characteristics and structure of natural patinas growth on artifacts. Nowadays the storage of bronze artifacts has received extensive attention. One of the most serious problems facing the conservators and conservation scientists is how to stabilize bronze artifacts against further corrosion under unfavorable environmental conditions. In order to improve conservation methods and provide more data to help the conservation scientists and conservators to control and stop the process of deterioration of ancient and historic metals in museums or in storage conditions, it is necessary to investigate the effects of air-pollutants on the corrosion of bronze. Actually, the synergistic effect of NO_2 and NaCl particles on bronze has been studied by Eriksson et al in their work published in Corrosion Science [12]. This work had been done in 90% RH and synergistic effect on the NaCl induced atmospheric corrosion of bronze was obtained with the combination of NO_2 and NaC1. However the corrosion behavior of bronze in NO_2+Cl- polluted air with a RH lower than 80% had been scarcely studied. In this paper, the effects of chloride together NO_2 on the atmospheric corrosion

JCSE The Journal of Corrosion Science and Engineering
ISSN 1466-8858 Volume 11, Preprint 35 submitted 11 December 2008

of bronze was studied by means of gravimetry, electrochemical technology and surface tension test as well as other analytical techniques. The main purpose is to study the simultaneous interaction of NO_2+Cl^- on the atmospheric corrosion of bronze.

2. Experimental

2.1 Preparation of specimen

Table 1 listed the chemical composition of bronze. The specimens were sectioned into ϕ 50mm×2mm, grounded with 150-grit silicon carbide paper and finished with 600-grit paper, ultrasonically washed in acetone and methanol, sequentially, then quickly dried and kept in a nitrogen atmosphere prior to the test.

Table 1 Chemical composition of bronze.

Cu %	Sn %	Pb%
75%	20%	5%

NaCl was deposited by the following procedure: A saturated solution of NaCl in 99.5% ethanol (C_2H_5OH) were taken and well distributed onto the bronze surface using a transfer pipette. The ethanol volatilized, whereby NaCl partials remained. Two different amounts of NaCl deposition (0.0; 120μg.cm^{-2}) were investigated. The samples were exposed in an air charger with 75% relative humidity and temperature at 20℃ in the present of 400 ppm NO_2 and in the absent of NO_2 respectively. The experiment lasted four weeks. During the exposure test, three samples were interrupted once a week and weighed with sensitivity better than to 0.1mg.

Surface tension tests were accomplished by a video frequency optical contact angle device

ISSN 1466-8858 Volume 11, Preprint 35 submitted 11 December 2008

(OCAZO). The effects of the Cl^- and NO_2 on the interfacial tensions were determined by measuring the respective contact angles of their forming solutions on the specimen. To make the macro size solution droplet, 10-100µl water was put onto the metal respectively after one day exposure using a suitable micro-syringe. Macro size droplets with the diameter of 0.5–5 mm were placed onto a metal specimen. The edge of the droplet and the region surrounding it were observed carefully by a laser microscope.

An M398 corrosion measurement system manufactured by EG&G was used to undertake electrochemical impedance (EIS) measurements. A Princeton flat cell three-electrode system was selected in which the reference electrode was a saturated calomel electrode (SCE), and the counter electrode was a platinum foil. The exposed area of specimens was 10mm × 10mm. A sine wave amplitude of 10mV and a frequency range of 100kHz-10mHz was used.

The study of corrosion products was performed by using SEM and X-ray diffraction (PW1700). SEM observations were made by using a Philips 515 microscope, which was coupled with a 9100 EDAX for surface analysis. SEM and EDAX data were used to characterize the morphology and chemical heterogeneities of the corrosion products. Full X-ray diffraction patterns were recorded for general identification of corrosion products between 10 and 90° two-theta.

3. Results

3.1 Weight loss measurements

Corrosion rates of the bronze specimens were determined by using weight loss measurement. Corrosion rates were only recorded when the specimen had already been uniformly corroded.

JCSE The Journal of Corrosion Science and Engineering
ISSN 1466-8858 Volume 11, Preprint 35 submitted 11 December 2008

Variation of the weight-loss of samples is shown in figure1.

.

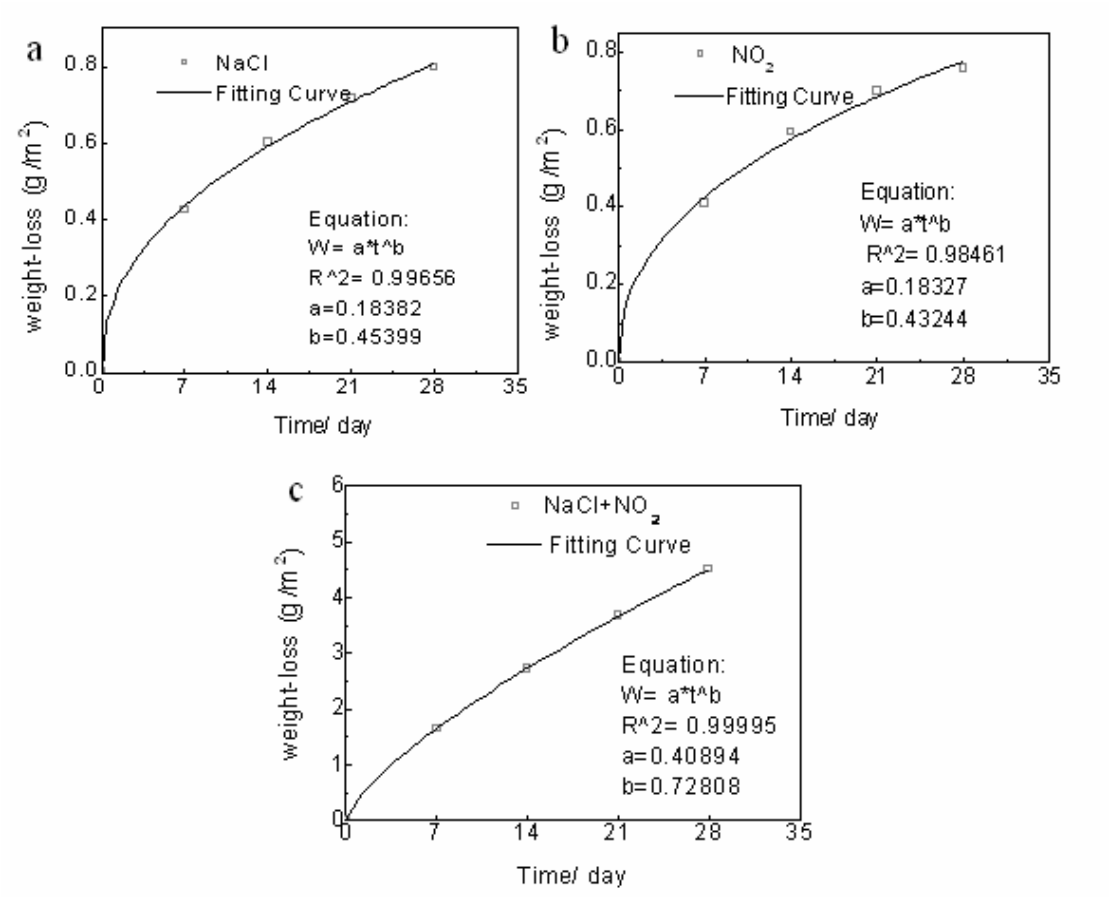

Fig.1 Weight loss curves of samples: (a) pretreated with NaCl in pure air, (b) untreated with NaCl in the present of NO_2 (c) pretreated with NaCl in the present of NO_2

The corrosion data are observed to approximately follow a bi-logarithmic equation:

$$W = at^b \quad (1)$$

Where W is the weight loss (g), t is the exposure time (day), and 'a' and 'b' are constants. It is clear that 'a' is equivalent to the weight loss when time is one hour. 'b' reflects the change in weight loss with time. The regression coefficients and the associated correlation coefficient (R^2) of the corrosion data from the weight-loss method is shown in figure 1 too.

For the main it is clearly observed from figure 1 that the weight-loss induced by $NaCl+NO_2$

ISSN 1466-8858 Volume 11, Preprint 35 submitted 11 December 2008

is the highest during the corrosion process of the test, and followed by those induced by NaCl and NO_2. The corrosion rate of samples pretreated with NaCl in pure air is of the same order as in the single NO_2 gas experiment. The value of 'a' induced by NaCl+NO_2 is higher than total of that induced by NaCl and NO_2. The corrosion rate induced by NaCl +NO_2 is little higher than total of that induced by NaCl and NO_2 at the initial corrosion stage and about 5 and 6 times higher with the corrosion proceeding. Thus a strong synergistic effect of simultaneous interaction of NO_2^- + Cl^- with bronze was observed. It is well known that constant 'b' is roughly equal to 0.5 of the corrosion which is controlled by an ideal diffusion process; if the value of 'b' is greater than 0.5, the corrosion is faster than the diffusion process, since the rust has been detached by cracking, erosion, dissolution, etc. If the value of 'b' is smaller than 0.5, it means a decrease in diffusion coefficient and the rust layer become more protective. Thus according to the value of 'b' showed in Figure 1, the corrosion layers induced by NaCl +NO_2 is very defective, and the rust layer induced by the NO_2 and NaCl is more protective than that induced by the NO_2+NaCl solution.

3.2 Surface tension test

The corrosion of bronze depends to a great extent on the make-up of the electrolyte in contact with the metal. Ion adsorption on the interface between electrode and solution has significant effects on the kinetics of electrode processes. Different ions have different adsorption abilities. Most inorganic anions obey typical ion adsorption rules because anions are generally surfactants. The adsorption of anions can change not only the electrode surface states but also the electric double layer distribution. Moreover, it can affect both the concentration of the reactants and the reaction active energy on the electrode surface, thus the reaction rate changes even if the anions don't take part in any reaction. Surely the reaction dynamics will be directly affected when

JCSE The Journal of Corrosion Science and Engineering
ISSN 1466-8858 Volume 11, Preprint 35 submitted 11 December 2008

these ions participate in the reaction. The surface tension and adsorption ability can be quantified and compared by measuring the respective contact angles. Figure 2 shows the morphologies of the micro-size droplets on the specimen surfaces. Contact angles of the droplets on the three kinds of bronze specimens are showed in table 2. From these data, it can be seen that the adsorption inclination on bronze electrode is $NaCl+NO_2$ > $NaCl \approx NO_2$ which coincides with the result of weight loss at the initial stage. The deposition of NO_2 on the chloride specimen causes the surface tension decrease on the electrode interface. The increasing of the adsorption ability of the anions in the electrolyte leads to the increasing of the corrosion rate. It can probably be concluded that corrosion processes at the initial stage are largely dependent on the absorption ability of anions on the specimen.

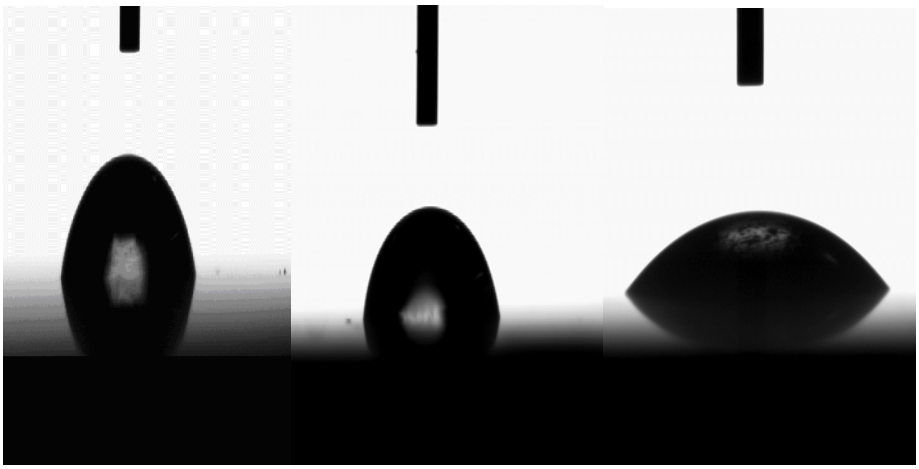

(a) (b) (c)

Fig.2 Micro photo of micro-droplets on the specimen: (a) NaCl (b) NO_2 (c) $NaCl+NO_2$

Table 2 Contact angles of the drop on the solution / bronze interface

NaCl	NO_2	$NaCl+NO_2$
88 °	*90 °*	42°

JCSE The Journal of Corrosion Science and Engineering
ISSN 1466-8858 Volume 11, Preprint 35 submitted 11 December 2008

3.3 Results of electrochemical Test

Electrochemical impedance measurements were performed to evaluate the protectiveness of the corrosion products formed after the exposure test. The impedance measurements were carried out in 0.01M NaCl+0.01M H_2SO_4 aqueous solution at the corrosion potential. The EIS data are showed in figure 3.

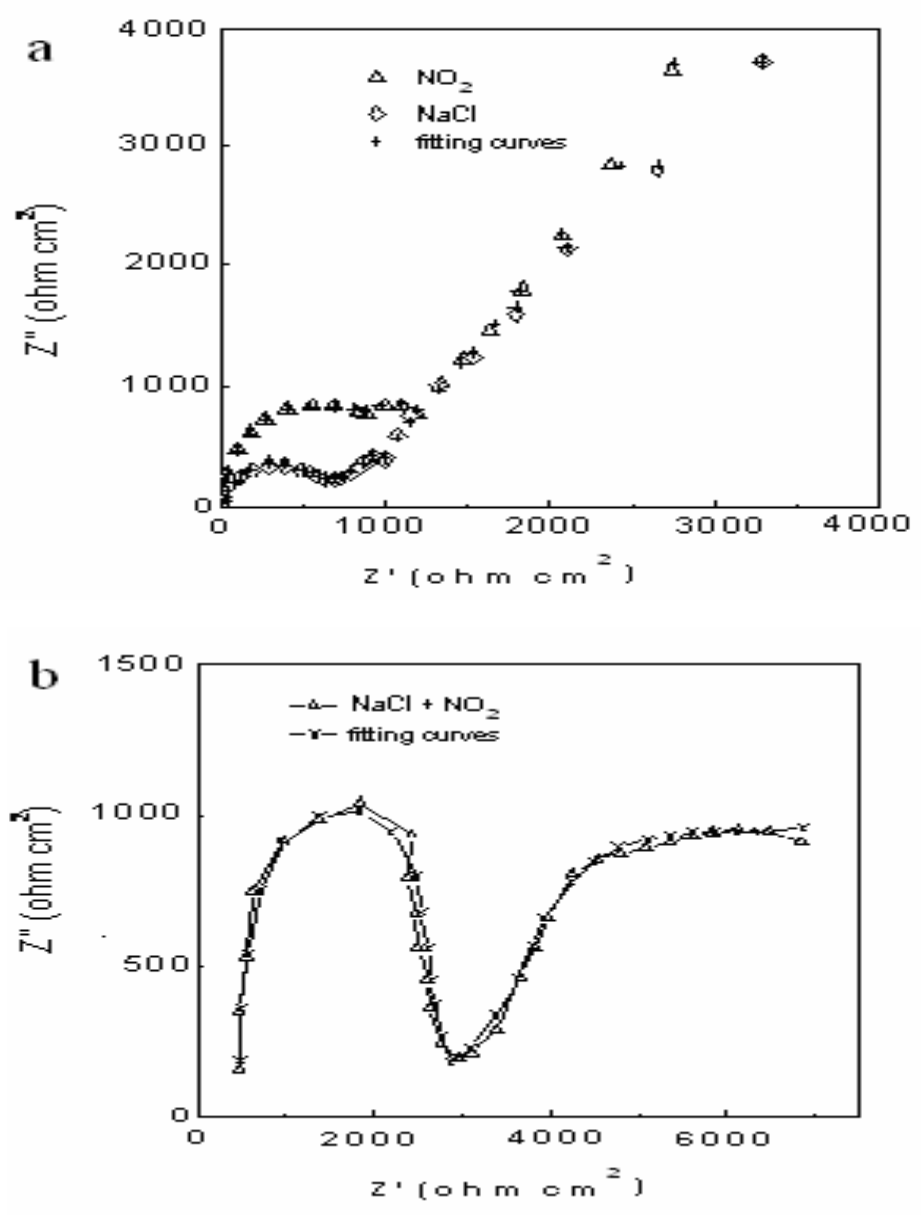

Fig.3 Experimental and simulated impedance spectra for the rusted specimen (a)by NO_2 and NaCl,

JCSE The Journal of Corrosion Science and Engineering
ISSN 1466-8858 Volume 11, Preprint 35 submitted 11 December 2008

(b) NO_2+NaCl.

It can be seen that the impedance spectrums induced by NO_2 and by NaCl exhibit a slightly distorted capacitive semicircles and a third contribution at very low frequencies, both LF parts of the impedance show the feature of Warburg impedance. The phase angle of the diffusion tail deviates from 45 degree, corresponding to slow processes occurring in the corrosion product layer such as diffusion. Since the passive films formed on bronze are usually described as bi-layered structures, the two time constants at higher frequencies can be associated with a compact Cu_2O inner layers and a porous outer layers, composed by cupric nitrate or chloride depending on the atmospheric pollutants. The experimental data can be discussed by taking into account the impedance of the two layer structure of the surface corrosion products in parallel with the cathodic reaction impedance, R_{cath} and an additional time constant for the mass transport contribution (Zw), and in series with the uncompensated ohmic resistance (R_Ω), according to the following transfer function:

$$Z(j\omega)= R_\Omega+\{[(j\omega C_{in} + R_{in}^{-1})^{-1} + (j\omega C_{ex} + R_{ex}^{-1})^{-1}]^{-1} + (R_{cath}+Zw)^{-1}\}^{-1} \quad (2)$$

Where C_{in} and R_{in} are the capacitance and resistance of the Cu_2O inner layer, respectively, and C_{ex} and R_{ex} are related to the contribution of the outer porous layer.

However the impedance spectrums induced by NaCl+NO_2 has the characteristics of double capacitive resistance arcs which can be interpreted by two time constant equivalent circuit model (Figure 4). This model is used to describing a rust layer with porosity in which electrochemical reactions may proceed, where R_1 is the solution resistance, Ra and Cd are the rust layer resistance and rust layer capacitance respectively: Cb is the double layer capacitance and Rb is the charge

ISSN 1466-8858 Volume 11, Preprint 35 submitted 11 December 2008

transfer resistance of a corrosion process.

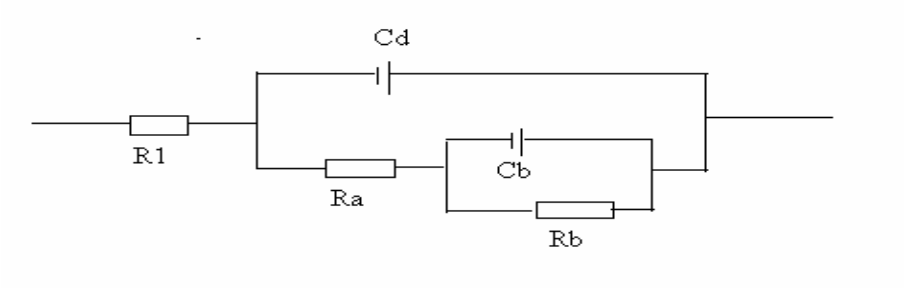

Fig. 4. Equivalent circuit of rusted samples in 0.01M NaCl+0.01MH_2SO_4 solution

For the each set of experimental impedance data, the parameters were fitted using a non-linear least-square method. Only the fit parameters R_{in} and R_{ex} and Ra which is related to the protectiveness of the rust layer are listed in table 3.

Table 3 shows that the total rust impedance value caused by the NO_2 is bigger, indicating a relatively better inhibition effect on the transfer of corrosion medium to the electrode surface, and thus providing better protection for the metal substrate. In contrast, the significant decrease in the value of rust impedance of rust layer induced by Cl^- indicated that the rust is not as protective. This shows agreement with the results of values 'b' in the weigh loss measurements which are less than 0.5. The rust layer induced by NO_2+NaCl is non-uninformed and defective, which show poor protection to substrate metal. This can be seen from the low value of Ra. The auto-catalysis effect and high mobility of Cl^- contribute to the formation cracks and flaws, which could give rise to local stresses, thereby chemically assisting the spread of cracks and the disintegration of the rust layers. In addition, no obviously laminated rusted layer induced by NaCl + NO_2 is observed. The whole rust layer is loose and defective, which can be attributed to the interaction among the corrosion product which inhibits the formation of the adherent inner layer of Cu_2O. This is agreement with the results of the value b in figure 1. The poor inhibition effect of the rust layer induced by NaCl and NO_2 is the results of the synergistic effect of chloride

ISSN 1466-8858 Volume 11, Preprint 35 submitted 11 December 2008

and NO_2.

Table 3 Values of R_{in} R_{ex} and Ra for rusted specimen induced by the solutions

	R_{in} (k . Ω)	R_{ex} (k . Ω)	Ra
NO_2	6.79	3.17	
NaCl	3.08	1.2	
NaCl+NO_2			2.4

3.4 Surface analysis techniques

SEM coupled EDAX analysis patterns were used for identifying the constituents of the rust layer formed on specimens after the exposure test as showed in figures 5. SEM analysis showed that the pattern of the corroded bronze samples from the three environments is quite different. Figure 5a: the lichen-like structure induced by NO_2 is copper hydroxide nitrate. Figure 5b: the crystal structure induced by NaCl are detected as rhombic paratacamite, In figure 5c the flakes crystal structure induced by NaCl+NO_2 is clearly showed which is the characteristic of aratacamite. The EDAX analysis showed that 'N' and 'Cl' was found in the corrosion product induced by NO_2 and by Cl^- respectively. However, it was worth noting that there is no "N' was found in the corrosion products that induced by NaCl+NO_2, and only much 'Cl' was detected. This also can be showed by the micro-crystal structure of the crystal of the corrosion product in the SEM pictures in figure 5c.

JCSE The Journal of Corrosion Science and Engineering
ISSN 1466-8858 Volume 11, Preprint 35 submitted 11 December 2008

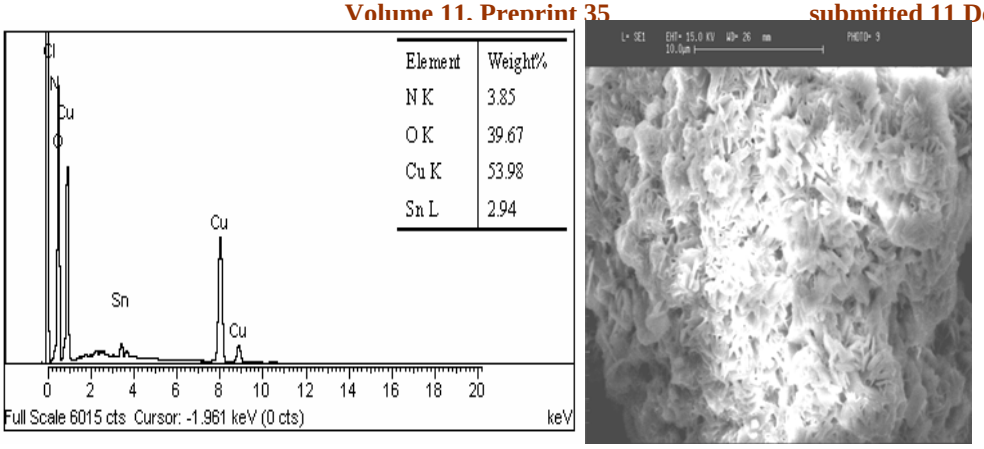

(a)

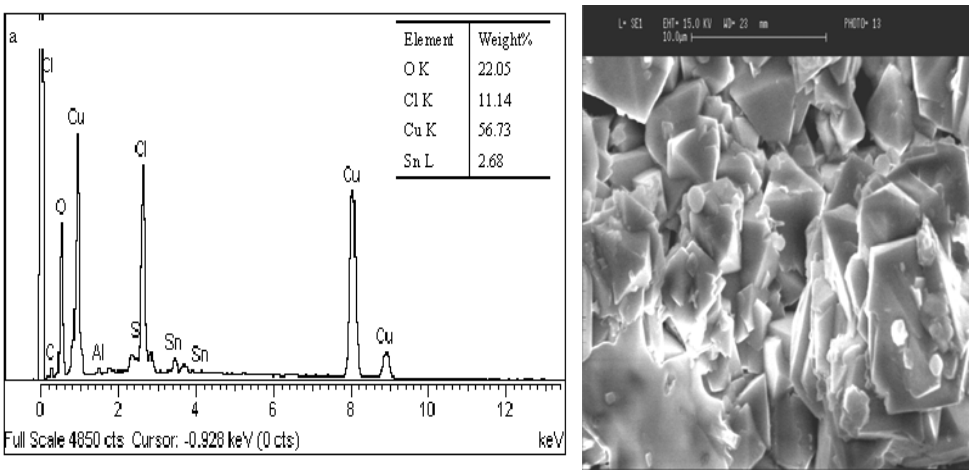

(b)

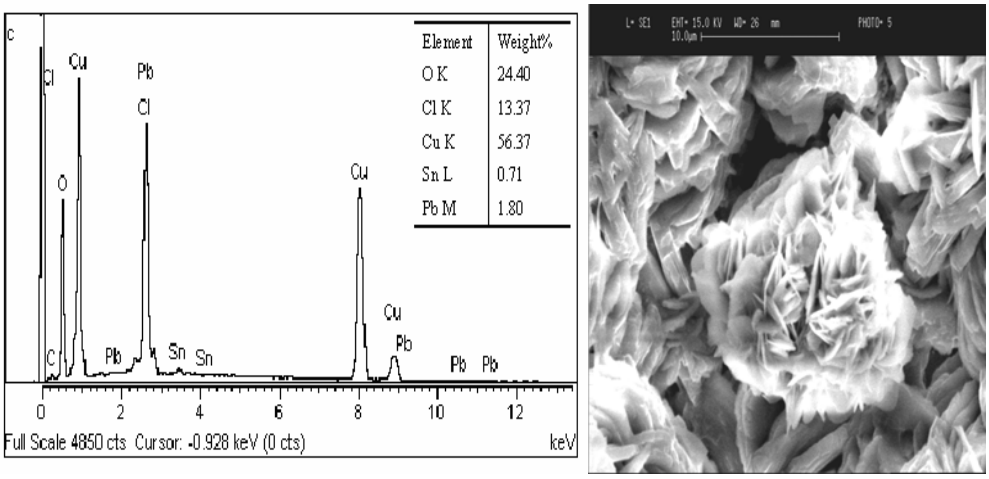

(c)

Fig. 5: SEM and EDAX analysis of the rust samples induced by (a) NO_2, (b) Cl^- and (c) Cl^-+NO_2

JCSE The Journal of Corrosion Science and Engineering
ISSN 1466-8858 Volume 11, Preprint 35 submitted 11 December 2008

3.5 The result of analysis using X-ray diffraction

The x-ray diffraction patterns recorded in the angular range of 10-90° 2θ were used for identifying corrosion product induced by the three environments. Typical diffraction patterns of corrosion products induced by the three different anions were shown in figure (6-8).

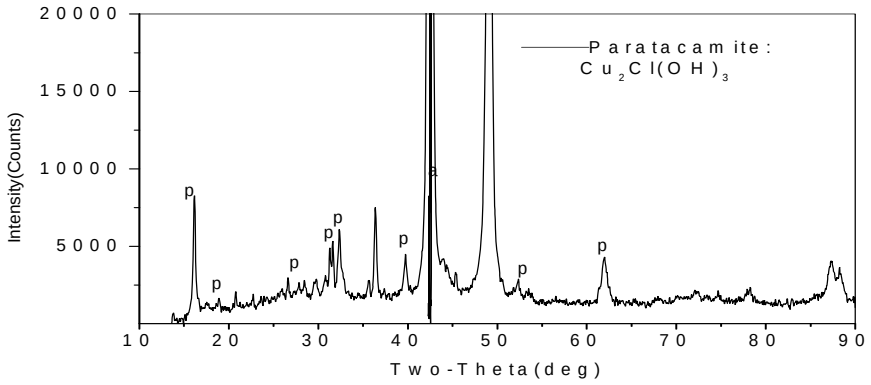

Fig.6. XRD patterns of bronze corrosion products formed on samples induced by Cl^- after exposure test.

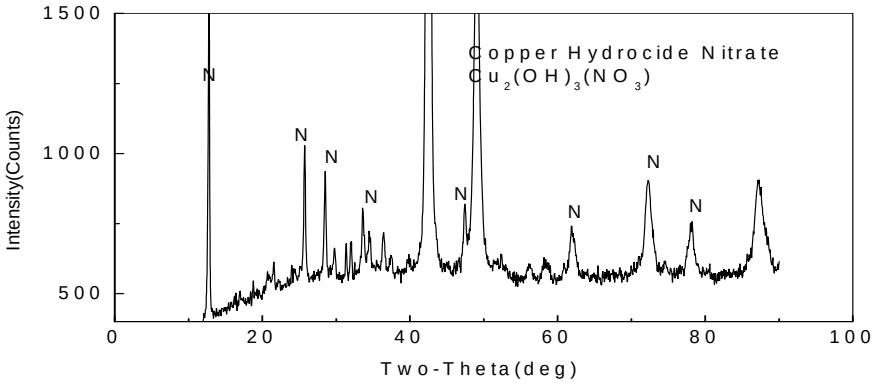

Fig.7. XRD patterns of bronze corrosion products formed on samples induced by NO_2 after exposure test

JCSE The Journal of Corrosion Science and Engineering
ISSN 1466-8858 Volume 11, Preprint 35 submitted 11 December 2008

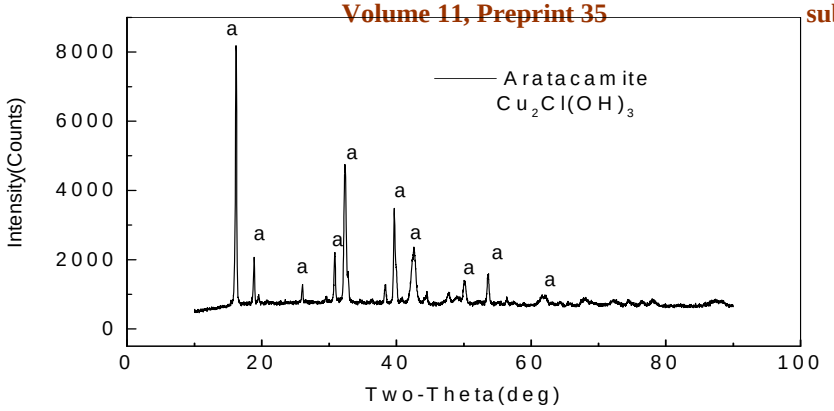

Fig.8. XRD patterns of bronze corrosion products formed on samples induced by Cl^-+NO_2 after test.

Patinas induced by chloride ion present vestiges of basic chorides of the type of nantolite (CuCl), also a large mount of paratacamite. Patinas induced by NO_2 after the exposure test present cuprite and copper hydrocide nitrate. However the most noting in the patinas constituents induced by Cl^-+NO_2 is only copper hydroxyl chloride and atacamite was found and no copper hydroxyl nitrate appears. This shows agreement with the result of EDAX analysis.

4 Discussions

Among the powdery rust, Sn is existed in the form of cassiterite (SnO_2), and Pb is in the form of PbO. These two kinds of oxide are very stable and have low solubility. They existed in the original place, and their corrosion processes are relative simple. The most complex corrosion process is the corrosion process of Cu, which is the greatest mount in the alloys.

4.1 The Effect of NO_2

When NO_2 is existed in the environment，the metal was oxidized, at meant time NO_2 is oxidized into HNO_3 which contribute to the formation of acid electrolyte. The corrosion process is

JCSE The Journal of Corrosion Science and Engineering
ISSN 1466-8858 Volume 11, Preprint 35 submitted 11 December 2008

accelerated. Owing to the relatively lower surface activity as figure 2 shows, the corrosion rate induced by NO_2 is relatively low at the initial corrosion stage. However, it is not that lower than that induced by Cl^- with the corrosion proceeding despite the inhibition of the rust layer induce by NO_2 is better as EIS result shows. It was proposed by Strandberg [13] that cuprite had the power to reduce NO_2 on the surface producing HNO_2. With the formation of cuprite, NO_2 is more inclined to be reduced. More nitrate corrosion product is formed with the corrosion progressing. This explains why the corrosion rate induced by NO_2 doesn't drop so fast in spite of the protection of the rust layer.

4.2 The Effect of Chloride

The deposition of NaCl on the surface of metal will accelerate the corrosion process. For one inspect, NaCl can adsorb the air-water from the atmosphere, and a electrolyte layer is formed on the metal. In addition, with the deposition of NaCl, the electrical conductivity of the electrolyte layer is increased. As figure 2 shows, Cl^- ion is famous for its exceptionally high surface activity which may make the surface tension on the metal relatively low. In the present case where Cl- is in the electrolyte, the following reaction occurs:

$$2Cu + 1/2O_2 + 2Cl^- + H_2O \rightarrow CuCl + 2OH^- \quad (3)$$

This reaction is very easy to occur in acid solutions.

$$CuCl + O_2 + 4H_2O \rightarrow 2Cu_2(OH)_3Cl + 2H^+ + 2Cl^- \quad (4)$$

Because the substrate metal is lack of oxygen, the reaction 2 is hampered. However, CuCl move outwards along the corrosive notch due to its minor solvency. The reaction occurred is as followed:

$$2CuCl + H_2O \rightarrow Cu_2O + 2Cl^- + 2H^+ \quad (5)$$

JCSE The Journal of Corrosion Science and Engineering
ISSN 1466-8858 Volume 11, Preprint 35 submitted 11 December 2008

It was argued that no matter how compact a passive layer contains flaws through which the chloride ions easily penetrates. The flaws were stated to be large enough to permit the passage of large aggressive ions. The role of chloride centers around: (a) competitive adsorption with OH- on the available copper surface thus creating sites that are more liable for electrochemical dissolution and (b) competition with OH- attached to Cu(Ⅱ) in a soluble intermediate stage, thus enhancing film rupture(through dissolution). Nevertheless, the degree of the influence of aggressive anions in breaking down protective films depends on both the nature of the surface (oxide) and the added anion. Then, although cuprous chloride can be formed in the surface film, the film rupture induced by the Cl- and its high mobility lead to the corrosion rate decreasing slowly.

4.3 The Combined Effect of Chloride and NO_2

Figure 2 have showed that the surface tension on the bronze/solution interface drop sharply on the specimen induced by NaCl +NO_2 contrasted with those induced by NaCl and NO_2. More Cl^- and NO_3^- are accepted at the electrolyte/metal interface. Corrosion is more inclined to occur. So the corrosion rate induced by Cl^-+ NO_2 is much higher than that induced by NO_2 at the initial corrosion stage. The synergistic effect occurs. With the corrosion progressing, the synergistic effect is still obvious as the weight loss result shows. It is worth noting that no "N" is found in the corrosion products as the results of both XRD and EDAX. Here a catalyst synergistic theory is recommended. That is the synergistic effect between Cl^-+ NO_2 which is processing by the catalysis of NO_2.

A general rule of catalytic reaction lies in: the catalysts reacts with the reactants forming a intermediated products, the reaction route changes, apparent activation energy is reduced. No

ISSN 1466-8858 Volume 11, Preprint 35 submitted 11 December 2008

change is happened on the characteristics of the catalysts. As the above has described in the present case where Cl^- is in the electrolyte, the reactions (3), (4) occur. And when NO_2 is coexisted in the environment，the metal was oxidized, at meant time NO_2 is oxidized into HNO_3., then under the cooperation of Cl- and NO_2, Copper hydrated chloride and NO occur. NO reacted with O_2 lead to the regeneration of NO_2. The reactions are as the following:

$$NO_2 + H_2O + O_2 \rightarrow HNO_3 \quad (6)$$

$$6CuCl + 2NO_3^- + 5H_2O \rightarrow 3Cu_2(OH)_3Cl + 2NO + 3Cl^- + H^+ \quad (7)$$

$$NO + O_2 \rightarrow NO_2 \quad (8)$$

At the normal condition when CuCl is present, the reactions （4）and (5) occurred. However when NO_2 is coexisted, the react (7) is accelerated. More atacamite is generated as figure 5 and figure 8 shows. There seems little paratacamite and cuprite occur in the rust layers (as XRD shows). This is due to the selectivity of catalyst. The existing of NO_2 may inhibit the formation of cuprite. As EIS shows, the protection of the rust layer induced by Cl^-+NO_2 is poor. This is one of the results of catalytic effect. A general patina evolution scheme of the copper in the alloys in Cl-+NO_2 environments is given in figure 9.

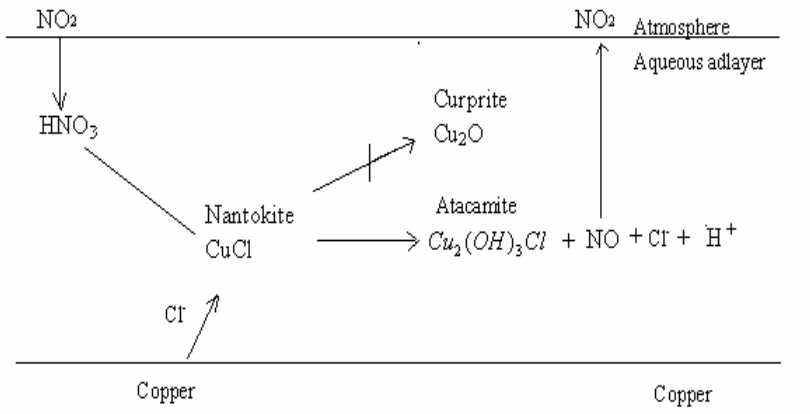

Fig. 9. A general patina evolution scheme of the copper in the alloys in Cl-+NO_2 environments

JCSE The Journal of Corrosion Science and Engineering
ISSN 1466-8858 Volume 11, Preprint 35 submitted 11 December 2008

The reaction between copper hydroxyl chloride and NO_2 implies the release of chloride ions and H^+ which create an acid electrolyte. The acidity of electrolyte aqueous will accelerate the solution of protective layer. In addition, the high penetration ability of Cl^- contributes to the rupture of the rust layer. As showed by the results of EIS, the rusted layer induced by NaCl + NO_2 is the very defective. The poor inhibition effect of the rust layer induced by NaCl + NO_2 is the results of the synergistic effect of chloride and sulfite ions too.

5 Conclusions

The experimental results showed that the attack to the metal at initial corrosion stage show great agreement with the surface activity of the ions that deposited on the metal. However as corrosion processed, the different reaction mechanisms and different characteristics of the corrosion products tend to dominant the corrosion process, which led to different changes on the corrosion rate.

A profound synergistic effect of combination of chloride +NO_2 ions was observed during the whole process. At the initial corrosion stage, it is chiefly due to the increasing of the adsorption ability of ions that deposited on it. However, the strong synergistic effect is still strong with the corrosion proceeding on. The following probably reasons could account for it: Ⅰ The acidity of electrolyte aqueous cause by NO_2 will accelerate the solution of protective layer, which will weaken the protection to the substrate. Ⅱ The high mobility and penetration power of Cl^-. Ⅲ NO_2 acted as a catalyst during the corrosion process when much chloride is coexisted.

Acknowledgements

This work was supported by The State Key Laboratory for Metallic Corrosion and Protection. Thanks are also extended to Panayota Vassiliou in National Technical University of Athens for

ISSN 1466-8858 Volume 11, Preprint 35 submitted 11 December 2008

her kindly help.

References

[1] J.Juan, S. Rodriyuez, Corrosion Science, 45, pp799-810, 2003.

[2] C. F. Lang, W. T. Hou, Corrosion Science, 7, pp183-196, 1995

[3] T. Kamimura, M. Stratmann, Corrosion Science, 43, pp429-441, 2001.

[4] W. Zhenyao, H. Wei, Transctions of Nonferror Metal Society of China, 17, pp326-339, 2007

[5] S. Oesch, M. Faller, Corrosion Science, 39, pp1505-1524, 1991

[6] A R. Mendoza, F. Corvo,Corrosion Science, 42, pp1123-1136, 2000

[7] C.Arroyave, F.A.Lopez, M.Morcillo, Corrosion Science, 37, pp1751-1761 , 1995

[8] C.Arroyave, M.Morcillo, Corrosion Science, 37, pp293-305, 1995

[9] S. J. Oh, D. C. Cook, H. E. Townsend, Corrosion Science, 41, 1687-1706, 1999

[10] Echavarría, A. Rueda, E. Cano, F. Echeverría, *C. Arroyave* and J.M. Bastidas, in: Proc. 15th Int. *Corrosion* Congress, Granada, Spain, (2002).

[11] CaoXia, Xu Chunchun Anti Corrosion and Protection , 52, pp 207-213, 2005

[12] P. Eriksson, L. G. Johansson and J. Gullman, Corrosion. Science, 34,1083-1097, 1993

[13] H. Strandberg, Atmosphere Environment, 20, pp3511-3520, 1998